XVI IMEKO World Congress
Measurement - Supports Science - Improves Technology - Protects Environment ... and Provides Employment - Now and in the Future
Vienna, AUSTRIA, 2000, September 25-28

CALIBRATION OF AE FOR TOOL WEAR MONITORING

A. Prateepasen, Y.H.J. Au and B.E. Jones
The Brunel Centre for Manufacturing Metrology
Brunel University, Uxbridge, Middlesex UB8 3PH, UK

Abstract: A calibration procedure using an air-jet as the artificial AE source was applied to single-point tool wear monitoring. The calibration procedure involves setting up an air-jet at a fixed stand-off distance from the top rake of the tool tip, applying in sequence a set of increasing pressures and measuring the corresponding AE. The root-mean-square value of the AE (AErms) obtained is linearly proportional to the pressure applied. This paper presents the results of machining tests and air-jet pressure test, both of which confirm that the tool system is linear with respect to AE propagation. Thus, irrespective of the layout of the sensor and AE source in a tool structure, AE can be expressed in terms of the common currency of 'pressure' using the calibration curve produced for that layout. Tool wear stages can then be defined in terms of 'pressure' levels.

Keywords: Calibration, Acoustic Emission, Single-point machining.

1 INTRODUCTION

Acoustic emission (AE) is the generation of stress waves created by the release of strain energy as a result of the material yielding under stress. In single-point metal machining, four different sources of AE, as shown in Figure 1, can be identified [1]:

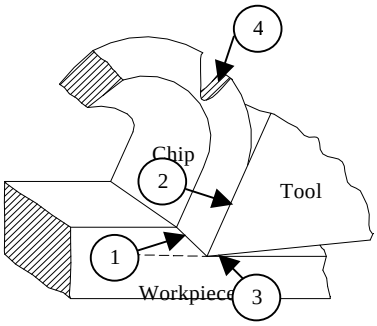

Figure 1. Four different sources of AE.

1. plastic deformation on the shear plane;
2. sliding friction and plastic deformation at the chip/tool interface;
3. sliding friction at the tool flank/workpiece interface; and
4. breakage of chips and their impact on the tool or workpiece.

Previous tool wear monitoring research has shown a direct correspondence between the energy or the root mean square value of the AE signal (AErms) and the different stages of tool wear [1-10]. The energy and AErms refer to the respective energy and root-mean-square value of the voltage output from the AE sensor. Models were proposed [1] that described the influence on the AErms of process variables in machining such as the feed rate, depth of cut and cutting velocity in single-point machining.

Modern machining uses indexable insert tools. An insert, clamped onto a tool-holder, is used to remove metal and when all its cutting edges are worn, a new insert is substituted. When monitoring tool wear using AE, the transmission characteristics of the tool between the tool tip and the sensor are exceedingly changeable. Not only is the sensed AE signal dependent on the geometry of the tool structure and the response characteristic of the sensor, it is also influenced by the subtle changes in the sensor and insert couplings with the tool holder, not to mention the effect of tool wear as observed by different researchers. As a result, AE data are hardly comparable between set-ups, making knowledge transfer very difficult, if not impossible.

To overcome the problem stated above, some form of calibration needs to be performed in order to establish the relationship between the AE measured by the sensor and the AE produced from a known reference source located on the tool tip. Two artificial AE sources, an air-jet and a pulsed laser, have been studied [11] and it is concluded that the air jet source had much in common with the AE produced during single-point machining. The comparison has been made between a reference AE source and a machining AE source based on the degree of likeness between the two frequency spectra of the respective AE signals using a measure called *similarity coefficient*. In addition, the air-jet source has the advantages that it is relatively safe compared to a laser source and that air is readily available in a machine shop.

In this paper, a calibration procedure using an air jet as the artificial AE source is described. The procedure establishes the relationship between the AErms and air pressure. The paper then presents evidence that the tool system (including the tool insert, tool holder, insert/tool holder coupling, sensor/tool holder coupling, and sensor) can be considered linear with respect to AE propagation so that an AErms value can be converted into a common equivalent value based on the pressure of the air jet.

2 COMPARISON OF SHAPES AND SIZES OF AE SPECTRA

An n-point RMS discrete spectrum can be thought of as a vector *u* defining a point in the n-dimensional vector space. By analogy with vectors in the three-dimensional space, the length squared of *u* is the inner product of *u* with itself. Thus, the length of *u* can be computed from

$$|u| = \sqrt{u.u} = \sqrt{\sum_{k=1}^{n} u_k^2} \qquad (1)$$

This length is the same as the AErms of the signal from which the n-point discrete spectrum is derived. The vector ***u*** can be normalised by dividing its elements by the length of the vector. A normalised vector, denoted by $\bar{u}$, has a unit length.

Given two normalised vectors, $\bar{u}$ and $\bar{v}$, in the n-dimensional space, the included angle *q* between them is related to the inner product of $\bar{u}$ and $\bar{v}$ as

$$\cos q = \bar{u}.\bar{v} . \qquad (2)$$

If the two vectors are identical, then *cosq* = 1, whereas if they are orthogonal to each other, meaning that the projection of one vector on the other is zero, then *cosq* = 0. Since the value of *cosq* suggests the degree of similarity between the two vectors, it is named the *similarity coefficient*.

Suppose there are *m* number of spectrum-vectors, u_1, u_2,..., u_m, to be compared, the individual lengths of these vectors can be computed by means of equation (1) and the corresponding normalised vectors obtained, namely, $\bar{u}_1$, $\bar{u}_2$, ..., $\bar{u}_3$. These normalised vectors, treated as column vectors, are then assembled into an n-by-m matrix *A* such that

$$A = (\bar{u}_1, \bar{u}_2, ..., \bar{u}_m). \qquad (3)$$

The similarity coefficient matrix *C*, by virtue of equation (2), is given by

$$C = A^T \cdot A \qquad (4)$$

where the element c_{ij} in C is the similarity coefficient between the spectrum-vectors u_i and u_j. It is noted that the matrix *C* is a symmetric matrix.

3 ARTIFICIAL AE AIR-JET SOURCE AND AIR PRESSURE

Calibration involves comparison between a reference source and a given source. Whereas comparison in one dimension is relatively straightforward, comparison in n-dimensions is not so easily defined. The method suggested is to consider an AE signal from the perspective of its RMS spectrum and then proceed to make comparison with the reference RMS spectrum in respect of its size and shape. The size relates to the strength of the signal whilst the shape corresponds to the distribution of the energy in the relevant frequency range. The size of a signal can be represented by the overall AErms of its spectrum. When comparing two signals to decide if they are similar in shape, the similarity coefficient can be used.

The air supply system that drove the air jet calibration rig is shown in the block diagram of Figure 2. A nozzle with a 1.0-mm diameter bore was placed normal to the rake face of the tool insert at a fixed distance of 5 mm. The centre of the air stream was positioned 2 mm from both the leading and trailing edges of the insert. The insert was clamped to the tool holder with a tightening torque of 2 Nm. The air pressure was varied from 5 to 8 bars in increments of 0.5 bar.

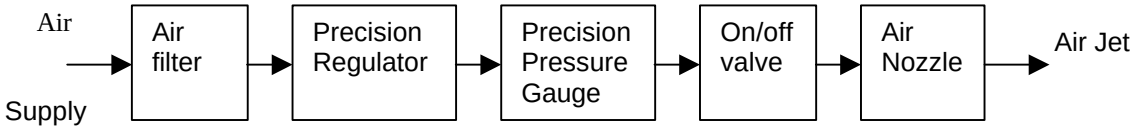

Figure 2. Block diagram of the air jet equipment.

A tool shank of type SDJCL 1616H 11 and carbide tool inserts of type CG 4035 DCMT 11 T3 04-UF (Sandvick Cormorant) were used. The detail of the insert geometry was as follows: insert shape 55°, clearance angle 7°, rake angle 0°, cutting edge length 11 mm, thickness 3.97 mm and nose radius 0.4 mm.

Two AE sensors were mounted on the tool-holder: a WD sensor (PAC) at the end of the tool-holder and an R30 sensor (PAC) on the side as shown in Figure 3. Both signals were amplified by 40 dB at the pre-amplifiers fitted with a 100 kHz – 1 MHz band-pass filter. The AE signals detected at the two sensors were analysed in real-time using a Hewlett Packard HP 89410A Vector Signal Analyser to produce a 401-line AErms spectrum spanning 0 to 1 MHz averaged over 70 consecutive spectra.

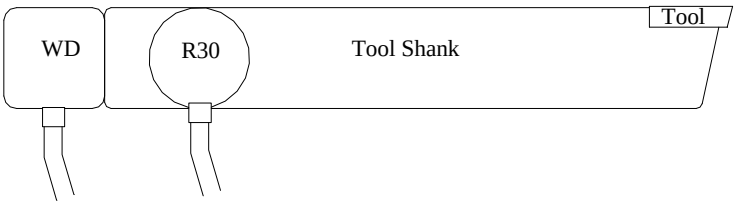

Figure 3. Two AE sensors (WD and R30) on the tool holder.

Typical AErms spectra of the air jet at the pressure of 5 bars obtained from the two sensors are shown in Figure 4. Their difference in shape is significantly due to the different frequency responses of the two sensors.

The AErms values of the air jet spectra obtained from pressures of 5 to 8 bars were computed using equation (1). The results from both the WD and R30 sensors are plotted in Figure 5. It can be seen that the AErms and air pressure are linearly related and the gradients for the WD and R30 sensors are 19.658 and 7.552 mV/bar respectively. These values represent the sensitivity of the two sensing systems.

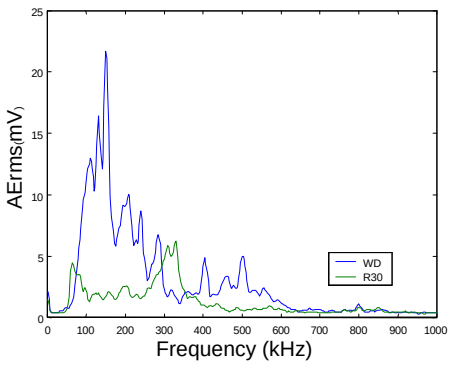

Figure 4. AErms spectra of the air-jet at the pressure of 5 bars.

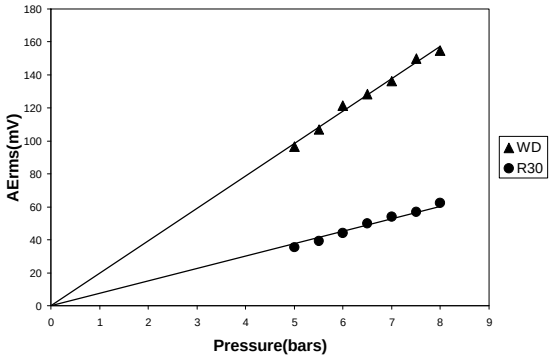

Figure 5. Relation between air-jet pressure and AErms.

The degree of likeness is computed using equation (4), returning the similarity coefficient matrix C for the WD sensor as

1	0.997	0.995	0.992	0.991	0.987	0.984
0.997	1	0.996	0.993	0.994	0.992	0.988
0.995	0.996	1	0.996	0.997	0.993	0.993
0.992	0.993	0.996	1	0.994	0.992	0.994
0.991	0.994	0.997	0.994	1	0.995	0.996
0.987	0.992	0.993	0.992	0.995	1	0.996
0.984	0.988	0.993	0.994	0.996	0.996	1

For the R30 sensor, the corresponding similarity coefficient matrix is given by

1	0.992	0.986	0.961	0.989	0.992	0.991
0.992	1	0.997	0.985	0.99	0.99	0.985
0.986	0.997	1	0.991	0.987	0.987	0.981
0.961	0.985	0.991	1	0.97	0.968	0.957
0.989	0.99	0.987	0.97	1	0.991	0.991
0.992	0.99	0.987	0.968	0.991	1	0.997
0.991	0.985	0.981	0.957	0.991	0.997	1

In these matrices, the rows and the columns represented the progressive pressure values of 5.0, 5.5, 6.0, 6.5, 7.0, 7.5 and 8.0 bars. It is evident from these matrices that the RMS spectra of a sensor are very similar to each other within this range of pressure as the coefficients are all very close to 1.

An RMS spectrum is simply the square root of the energy spectrum, also known as the spectral density function. In terms of the spectral density functions, the transfer characteristics from the air-jet input source to the output of the sensing instrument is governed by

$$G_y(f) = |H(f)|^2 \cdot G_x(f)$$

where the respective spectral density functions of the input and output are $G_x(f)$ and $G_y(f)$, and $H(f)$ is the frequency response function describing the dynamics of the signal transmission process which includes that of the tool and of the sensor. It should be noted that $G_x(f)$ denotes the AE produced at the tool tip as a result of the action of the air jet and not the air pressure itself.

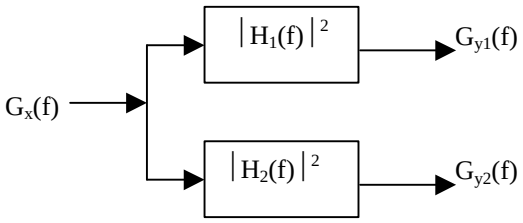

Figure 6. Different signal propagation paths with common input.

Figure 6 shows the different signal propagation paths with common input for the two different layouts of the WD and R30 sensors denoted by the respective subscripts of 1 and 2. Since the same input Gx(f) is used, their transfer equations can be written as

$$G_{y1}(f) = |H_1(f)|^2 \cdot G_x(f) \quad (5)$$

and

$$G_{y2}(f) = |H_2(f)|^2 \cdot G_x(f) \quad (6)$$

Dividing equation (5) by equation (6), we obtain

$$G_{y1}/G_{y2} = |H_1|^2 / |H_2|^2 \quad (7)$$

Figure 7 shows the ratio G_{y1}/G_{y2} for the range of air pressures from 5 to 8 bars with the curve of the mean ratio shown in bold solid line. The curves have been smoothed using the kernel smoothing technique. It is evident that all the curves are close to each other. According to equation (7), this suggest that the ratio of the frequency response functions, corresponding to the different sensors layouts, remain the same at any pressure within 5 to 8 bars. There are only two possible inferences from this: 1) that $H_1(f)$ and $H_2(f)$ are not affected by the input states of the air pressure, or 2) that both $H_1(f)$ and $H_2(f)$ are affected equally by the input states such that the resulting ratio remain constant. The second possibility is highly improbable, as it means that the condition must be maintained at all frequencies, 0 to 1 MHz, across the spectrum.

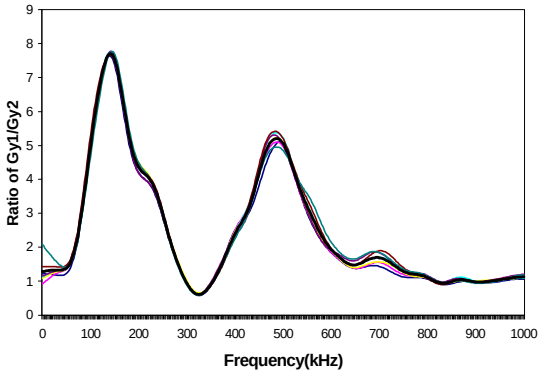

Figure 7. The ratio of G_{y1}/G_{y2} of air pressure from 5 to 8 bars.

Referring to either of equation (5) or (6), since neither $G_{yi}(f)$ nor $H_i(f)$ $(i=1,2)$ changes its shape with pressure, so will $G_x(f)$ retain its own shape. Thus, the sensitivity values of 19.658 and 7.552 mV/bar for the respective WD and R30 sensors apply not just to the overall AErms of the total signal, but also to the individual spectral components too.

Whilst the theory presented proves adequate for AE signals produced by the air jet with 5- to 8-bars of pressure, the AE produced from machining is much stronger and so the question of whether the calibration as described can be applied to the machining process needs to be answered.

4 AE FROM SINGLE-POINT MACHINING

The instrumentation used for the machining tests was identical to that for the air-jet calibration except that the total gain of the sensor output was 34 dB instead of 40 dB. It was necessary to use a lower gain in order to avoid saturation of the signal.

Three sets of machining tests were conducted and their conditions are detailed in the following:

- Machining Test Set 1: Variable feed rates from 0.05 mm/rev to 0.4 mm/rev in increments of 0.05 mm/rev. Cutting speed and depth of cut were constant at 120 m/min and 0.75 mm respectively.
- Machining Test Set 2: Variable speeds from 80 m/min to 150 m/min in increments of 10 m/min. Feed rate and depth of cut were constant at 0.2 mm/rev and 0.75 mm respectively.
- Machining Test Set 3: Variable depths of cut from 0.3 mm to 1.0 mm in increments of 0.1 mm. Cutting speed and feed rate were constant at 120 mm/min and 0.2 mm/rev respectively.

The material of the workpiece, measured 63.5 mm in diameter and 150 mm in length, was EN24T with 0.35-0.45 %carbon. All tests were conducted on a Traub lathe.

The ratios of G_{y1}/G_{y2} for the three sets of machining tests were first obtained and then the mean ratios for each set were calculated. The mean ratios for the three different machining conditions and for the air jet calibration are shown in Figure 8.

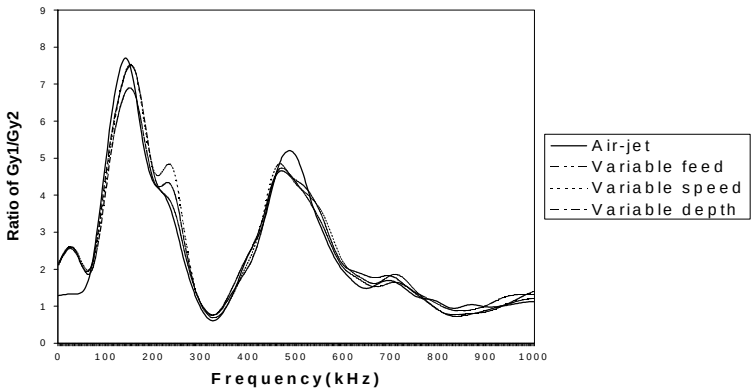

Figure 8. The ratios of G_{y1}/G_{y2} for the three sets of machining tests.

It can be observed that these curves match each other very closely. The implication is that the frequency response functions $H_1(f)$ and $H_2(f)$ in equations (5) and (6) are insensitive to the input states, whether they be caused by air-jet pressure or by machining.

5 CALIBRATION PROCEDURE

Based on the results presented, a simple calibration procedure for AE in machining studies is proposed. Using the air-jet artificial AE source set up under the conditions as stipulated in this paper, the AErms output of a sensor is measured over the range of air pressures from 5 to 8 bars. The sensitivity is then calculated from the gradient of the straight line fitted to the data points similar to Figure 5. With the sensitivity value known for a given layout of the AE sensor, the sensor output can then be converted into the pressure unit in bars. This unit is the common currency which forms the basis for comparison between results obtained with different sensor layouts or coupling conditions.

6 CONCLUSIONS

A number of conclusions can be made from the work. First, the frequency spectra of the AE produced by the air jet and machining were very similar to each other. Secondly, the frequency response function of the tool/sensor system was purely a function of the frequency and was independent of the input states or input mechanisms such as produced by air pressure or machining. Thirdly, using the calibration as prescribed, it is possible to convert an AErms value into an equivalent air-jet pressure value.

With the proposed calibration, it will be possible to make comparison between results obtained from different set-ups. This is, hopefully, a first step towards the building up of a meaning knowledge base on tool wear monitoring using AE.

ACKNOWLEDGEMENTS

The authors wish to acknowledge support from the INTErSECT Faraday Partnership, the Engineering and Physical Sciences Research Council and the Royal Thai Government.

REFERENCES

[1] R.Teti, D.A. Dornfeld, Modelling and experimental analysis of acoustic emission from metal cutting, *Trans. ASME, Journal of Engineering for Industry*, **111** (3) (1989) 229-237.
[2] E.N.Diei, D.A.Dornfeld, A model of tool fracture generated acoustic emission during machining, *Trans. ASME, Journal of Engineering for Industry*, **109** (3) (1987) 227-234.
[3] E. Kannatey-Asibu, Jr. and D.A. Dornfeld, Quantitative relationships for acoustic emission from orthogonal metal cutting, *Journal of Engineering for Industry*, **103** (3) (1981) 330-340.
[4] L. Dan, J.Mathew, Tool wear and failure monitoring techniques for turning-a review, *Int J.Mach.Tools Manufact*, **30** (4) (1990) 579-598.
[5] M.S .Lan, D.A. Dornfeld, In-process tool fracture detection*, Journal of Engineering Materials and Technology*, **106** (2) (1984) 111-118.
[6] T.Blum, I. Inasaki, A study of acoustic emission from the orthogonal cutting process, *Trans. ASME, J. Engineering for industry*, **112** (1990), 203-211.
[7] A.E. Diniz, J.J. Liu and D.A. Dornfeld, Correlating tool life, tool wear, and surface roughness by monitoring acoustic emission in finish turning, *Wear***, 153** (1) (1992) 396-407.
[8] J.J. Liu, D.A. Dornfeld, Modelling and analysis of acoustic emission in diamond turning, *Journal of Manufacturing Science and Engineering*, **118** (1996) 199-206.
[9] T.A. Carolan, S.R. Kidd, D.P. Hand, S. J. Wilcox, P. Wilkinson, J.S.Barton, J.D.C. Jones and R.L. Reuben, Acoustic emission monitoring of tool wear during the face milling of steels and aluminium alloys using a fibre optic sensor, part1: energy analysis, *Proc Instn Mech Engrs*, **211** (1997) 299-309.
[10] K.Iwata, T. Moriwaki, An application of acoustic emission measurement to in-process sensing of tool wear*, Annals of the CIRP*, **26** (1)(1977) 21-26.
[11] A. Prateepasen, Y. H. J. Au and B.E. Jones, Comparison of artificial acoustic emission sources as calibration sources for tool wear monitoring in single-point machining*, "Proceedings of the 24th European Conference on Acoustic Emission Testing*" (Senlis, 24-26. May 2000), CETIM, France, 2000.

Contact: Professor B. E. Jones, The Brunel Centre for Manufacturing Metrology
Brunel University, Uxbridge, Middlesex UB8 3PH, UK